https://doi.org/10.5194/se-2021-117
Preprint. Discussion started: 30 September 2021

Solid Earth
Discussions
Open Access

Interpolation of magnetic anomalies over an oceanic ridge region using an equivalent source technique and crust age model constraint

Duan Li[1], **Jinsong Du**[1,2], **Chao Chen**[1], **Qing Liang**[1], **and Shida Sun**[3]

[1] Hubei Subsurface Multi-scale Imaging Key Laboratory, Institute of Geophysics and Geomatics, China University of Geosciences, Wuhan 430074, China

[2] State Key Laboratory of Geological Processes and Mineral Resources, China University of Geosciences, Wuhan 430074, China

[3] Hebei Key Laboratory of Strategic Critical Mineral Resources, Hebei GEO University, Shijiazhuang 050031, China

Correspondence: Jinsong Du (jinsongdu@cug.edu.cn)

https://doi.org/10.5194/se-2021-117
Preprint. Discussion started: 30 September 2021

Solid Earth
Discussions
Open Access

Abstract. Marine magnetic surveys over oceanic ridge regions are of great interest for investigations of structure and evolution of oceanic crust, and have played a key role in developing the theory of plate tectonics (Dyment, 1993; Maus et al, 2007; Vine and Matthews, 1963). In this study, we propose an interpolation approach based on the dual-layer equivalent source model for the generation of a magnetic anomaly map based on sparse survey line data over oceanic ridge areas. In this approach, information from an ocean crust age model is utilized as constraint for the inversion procedure. The constraints can affect the magnetization distribution of equivalent sources following crust age. The results of synthetic tests show that the obtained magnetic anomalies have higher accuracy than those obtained by other interpolation methods. Meanwhile, considering the unclear on the true magnetization directions of sources and the background field in the synthetic model, well interpolation result can still be obtained. We applied the approach to magnetic data obtained from five survey lines east of the Southeast Indian Ridge. This prediction result is useful to improve the lithospheric magnetic field models WDMAMv2 and EMAG2v3, in the terms of spatial resolution and the consistency with observed data.

Plain Language Summary

Magnetic anomalies caused by rocks on the seafloor in mid-ocean ridge regions may reveal the evolution of oceanic crust and future of seafloor spreading, dynamic state of the mantle. However, marine magnetic surveys are generally carried out using only few survey lines and thus there are many areas with data gaps. The lack of data affects the identification and interpretation of magnetic anomalies. Traditional interpolation methods based on the morphological characteristics of data, such as kriging, minimum curvature, or the spline function, are not suitable for data with large gaps. Equivalent sources replacing real sources can be used to produce a better magnetic field prediction. In this study, we used the dual-layer equivalent source model to identify marine magnetic anomalies at the Southeast Indian Ridge. The synthetic tests show that the resolution and accuracy of our approach are higher than other methods and the prediction derived from observed data can improve other lithospheric magnetic field models.

Keywords

Data interpolation, Marine magnetic anomaly, Dual-layer equivalent source method, Magnetic lineation, Constraint, Ocean crust age model

https://doi.org/10.5194/se-2021-117
Preprint. Discussion started: 30 September 2021

1 Introduction

Marine magnetic anomalies provide critical evidence for the evolution of the seafloor (Granot and Dyment, 2019; Tontini et al., 2019; Bowles et al., 2020; Maher et al., 2020) and detailed information on plate tectonics(Sager et al., 1998; Sayanagi and Tamaki, 1992; Tominaga et al., 2008; Granot et al., 2012; Demirel et al., 2020). Data from observations revealed "stripe" features of magnetic anomalies in the oceanic ridge region, that is, magnetic lineation, providing information about the seafloor spreading history (Vine and Matthews, 1963). However, in many regions, there is a lack of survey lines or they are sparsely distributed. Insufficient data may cause ambiguity in identified magnetic anomalies, especially with respect to the lateral extension of the magnetic lineation. A magnetic map based on observed data can be a convenient way to show the features of these magnetic anomalies. It is also useful for additional data processing and the interpretation of the whole region. Therefore, an effective approach for data interpolation is required.

Traditional interpolation techniques based on the morphological characteristics of data, such as kriging (e.g., Krige, 1951; Hansen, 1993), minimum curvature (MC; e.g., Briggs, 1974), cubic spline interpolation (CSI; e.g., Meshram et al., 2018), and inverse distance weighting (IDW; e.g., Shahbeik et al., 2014), have been widely used. However, these methods might not be optimal for the data prediction in areas with insufficient data. In theory, the magnetic field can be interpolated by constructing a local magnetization model. Dampney (1969) proposed an equivalent source (ES) method to convert gravity anomalies using discrete observation data. The ES techniques, which reduce the difficulty of modeling by using a set of virtual sources, have been used for the interpolation of gravity and magnetic fields (e.g., Cordell, 1992; Cooper, 2000). This type of approach may provide a more accurate magnetic

https://doi.org/10.5194/se-2021-117
Preprint. Discussion started: 30 September 2021

field by improving the structure and distribution of the ES (Li et al., 2020). Thus, the ES technique may be suitable to obtain a reasonable interpolation of magnetic anomalies in oceanic ridge regions.

An ES model generally consists of a set of small bodies with uniform sizes that are placed beneath the observation surface. The model is used to generate a magnetic field that agrees with the observed data and a regional magnetic map is created. The magnetic properties of the ES bodies are determined by inverting the observed magnetic data. If there is a lack of observation data, prior information from geological investigations, such as the seafloor relief or oceanic crust age, can be used as constraint for the inversion. The constrained inversion allows the creation of realistic magnetization distributions of the ESs. It is conducive to predicting magnetic anomalies in areas with data gaps. In previous studies of the constrained inversion of potential field data, many techniques were proposed with respect to the introduction of constraints (e.g., Lelièvre and Oldenburg, 2009; Paoletti et al., 2013; Sun and Chen, 2016). Ocean crust age data can be used as guidance for the inversion and to determine the magnetization distribution of the ESs. Maus et al. (2009) used an oceanic crustal age model to interpolate between sparse track lines by directional gridding, wherein the information of crust age constrain the magnetic anomalies by influencing the magnitude of anisotropy factors in gridding the field over whole region. This thought provides a good reference for the study of this paper, and compared with the algorithm based on the morphology of data, constructing a equivalent source model maybe more compliance the principle of magnetic field.

In this paper, a dual-layer ES approach was used to create a magnetic anomaly map for an oceanic ridge region. An oceanic crust age model (Müller et al., 2008) was utilized and data obtained from five survey lines in the east of the Southeast Indian

Ridge were used to create a magnetic anomaly map.

2 Methodology

Susceptibilities or magnetization intensities of discrete sources were obtained by the inversion of observed data. Regularization and precondition techniques were utilized to stabilize the inversion process and balance the decay of the potential field. The matrix equation can be written as:

$$\mathbf{P}(\mathbf{G}^{\mathrm{T}}\mathbf{G} + \lambda\mathbf{I})\mathbf{m} = \mathbf{P}\mathbf{G}^{\mathrm{T}}\mathbf{d}, \tag{1}$$

where **P** denotes the precondition matrix, which is diagonal (the diagonal element is the inverse of the depth weighting function; Li et al., 2020); **G** is the kernel function matrix; $\lambda\mathbf{I}$ is the identity matrix multiplied by the regularization factor λ; and **m** and **d** are the vectors of the susceptibility or magnetization intensity of the ES model and observed data, respectively. Li and Oldenburg (1996) suggested the introduction of an objective function for smoothing to solve the optimization problem and obtain a smooth physical property model. The objective function provides several parameters that can be selected for the addition of constraints. Based on the aim of our work, the model objective function should contain two items (Li and Oldenburg, 1996; see equation below). The model objective function can be written as:

$$\phi_m = \int_v w_x \left|\frac{\partial m}{\partial x}\right|^2 \mathrm{d}v + \int_v w_y \left|\frac{\partial m}{\partial y}\right|^2 \mathrm{d}v, \tag{2}$$

where w_x and w_y are the flatness values between adjacent cells of the model in two different horizontal directions, respectively. By altering the relative values of w_x and w_y, the inverted model is smoothed or unsmoothed. For instance, if the flatness w_x is larger, the recovered model is elongated in the x-direction. If a larger flatness is assigned to a cell in the ES model, which is composed of a set of discrete and

https://doi.org/10.5194/se-2021-117
Preprint. Discussion started: 30 September 2021

contiguous cells, smooth lateral variations in the physical properties of adjacent cells are enforced. In contrast, assigning a smaller flatness to a cell leads to prompt variations in the physical properties of adjacent cells. By setting w_x and w_y, a constraint model can be constructed. After discretizing Eq. (2) and adding weights to the objective function, Eq. (1) can be rewritten as follows:

$$\mathbf{P}[\mathbf{G}^{\mathrm{T}}\mathbf{G} + \lambda(\mathbf{W}_x^{\mathrm{T}}\mathbf{W}_x + \mathbf{W}_y^{\mathrm{T}}\mathbf{W}_y)]\mathbf{m} = \mathbf{P}\mathbf{G}^{\mathrm{T}}\mathbf{d}\,, \tag{3}$$

where $\mathbf{W}_x$ and $\mathbf{W}_y$ are flatness matrixes in two horizontal directions, respectively.

In this study, an ES model was assembled using two layers at different depths. A shallow layer was placed on a surface below the seafloor with a constant depth difference based on the suggestion of Xia et al. (1993). Weights were only assigned to ES cells in the shallow layer. A layer with larger ES cell sizes at larger depth was utilized to simulate the background magnetic field.

Because the oceanic crust age and magnetic lineation in an oceanic ridge region correlate, the variation of the oceanic crust age can be inferred based on the variations of the magnetic properties (magnetization intensity or direction) of crustal rock. During cooling, the crustal rocks are magnetized by the geomagnetic field. The remanent magnetization of the crustal rocks reveals the variation of the paleomagnetic field. The long-term variation of the geomagnetic field can be generally divided into quiet variation and pole reversal. The pole reversal period is generally much shorter than the quiet variation. Because magnetic anomalies caused by crustal rocks that formed during a certain period have similar features, we can classify the magnetization characteristics of crustal rocks based on the oceanic crust age and the oceanic crust age can be used as constraint.

To add constraints, we can firstly extract the dividing lines of crust age from an oceanic crust age model using edge extraction techniques (e.g., Cooper and Cowan,

https://doi.org/10.5194/se-2021-117
Preprint. Discussion started: 30 September 2021

2008), which indicates the mutation of magnetized intensity or direction. Subsequently, a smaller flatness is assigned to the ES cells of the belt. A larger flatness is assigned to cells in the zones between dividing lines with relatively smooth magnetization variation. A smaller or larger flatness represents weights making the variation of cell's magnetic property discontinuous or continuous. Based on previous work (e.g., Lelièvre and Oldenburg, 2009; Paoletti et al., 2013; Sun and Chen, 2016), smaller flatness values are below 10^{-4}, larger flatness values are above 10^{4}, and normal flatness values (w_x = 1, w_y = 1) indicate that no weight was used (see Supplementary Material). Furthermore, the axis rotation can be used to transform w_x and w_y (Li and Oldenburg, 2000; Lelièvre and Oldenburg, 2009), if it is necessary in where kinks exist in the lineated anomalies.

3 Synthetic model experiment

A synthetic crust model consists of a set of north–south oriented horizontal prisms that are placed at a depth of 600 m (below the seafloor) to simulate the crust in mid-ocean ridge areas. Based on the pattern of seafloor spreading during different geologic ages, we assume that the prisms have different inclinations, thicknesses, and geological ages (each prism spanning one Mega year) and symmetrically extend from the mid-oceanic ridge axis outward. Considering that magnetic anomalies are generally caused by different sources at various depths, we used a stronger background magnetic field in this study and added it to the theoretical magnetic anomalies (Figure 1), which is forward by a randomly generated magnetic interface for simulating the unclear long-wavelength information in fact.

https://doi.org/10.5194/se-2021-117
Preprint. Discussion started: 30 September 2021

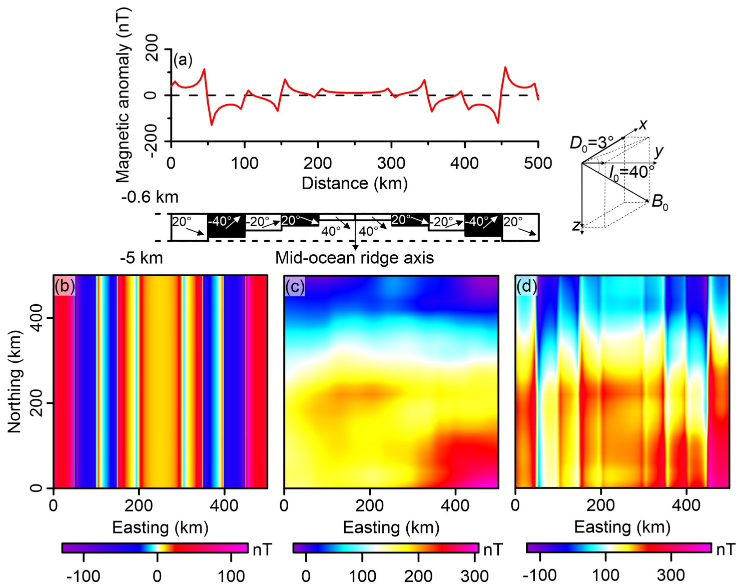

Figure 1. Synthetic model and magnetic anomalies at the sea level. (a) Magnetic anomaly and model for the west–east cross section. The black and white blocks represent the different assumed crust ages and associated remanent magnetization inclinations; (b) Magnetic anomaly in the study area generated by the model; (c) Simulated background magnetic field; (d) Total magnetic anomaly based on the combination of (b) and (c); the main geomagnetic field (B_0) has an intensity of 35000 nT and the inclination (I_0) and declination (D_0) are 40° and 3°, respectively.

Theoretical data for the thirteen survey lines in the east–west direction (perpendicular to oceanic ridges, at intervals of 50 km) were used for the inversion. Weight values of w_x = 10^4 (in the south–north direction) and w_y = 10^{-4} (in the east–west direction) were assigned to the cells on the edges (Figure 2a) of age stripes in the model (Figure 1a). Weight values of $w_x = 10^4$ and $w_y = 1$ were assigned to other cells to enforce their magnetic properties in the south–north direction during the inversion procedure. We utilized the preconditioned conjugate gradient (PCG)

https://doi.org/10.5194/se-2021-117
Preprint. Discussion started: 30 September 2021

technique to solve the inversion problem. The magnetic anomaly map generated based on our method agrees well with the theoretical data with respect to the survey lines and whole region (Figure 2b). Relatively large errors can be observed in several belts between survey lines, which are due to the effect of the background magnetic field. For comparison, we employed kriging, MC, IDW, and CSI to interpolate the survey line data. The magnetic maps generated based on these methods exhibit notable misfits in areas with data gaps (Figures 2c–f).

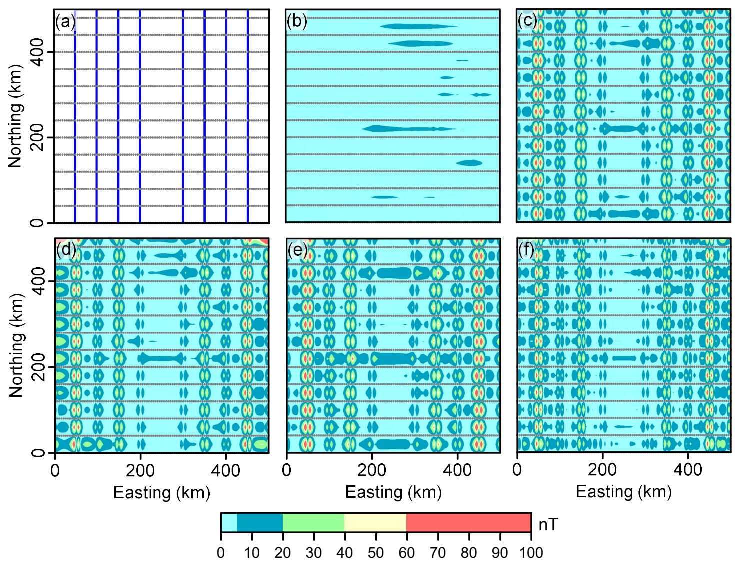

Figure 2. Results obtained with the model and comparison. (a) Distribution of the weighted ES cells (blue) on the prism edges and data from 13 survey lines (grey) selected for inversion; (b), (c), (d), (e), and (d) are absolute errors in the generated magnetic anomaly maps relative to theoretical data based on the use of our method, kriging, MC, IDW, and CSI.

4 Real data example

In this study, we used marine magnetic observation data acquired in the east of the

https://doi.org/10.5194/se-2021-117
Preprint. Discussion started: 30 September 2021

Southeast Indian Ridge (131°–136° E and 51°–55° S; Figure 3a). Data with an average spacing of ~1.5 km were collected from five survey lines. After leveling and removing the core and external fields, total-field magnetic anomaly (ΔB) data were obtained (Quesnel et al., 2009; Figure 3b). For calculation and drawing purposes, we transformed the raw data in spherical coordination into Cartesian coordinates. The crust age data in the study area (Figure 3c) were extracted from the global oceanic crust age model (Müller and Sdrolias, 2008) and the average inclination and declination of the main geomagnetic field (–82.12° and 2.27°, respectively) were obtained from the IGRF12 (Thébault et al., 2015).

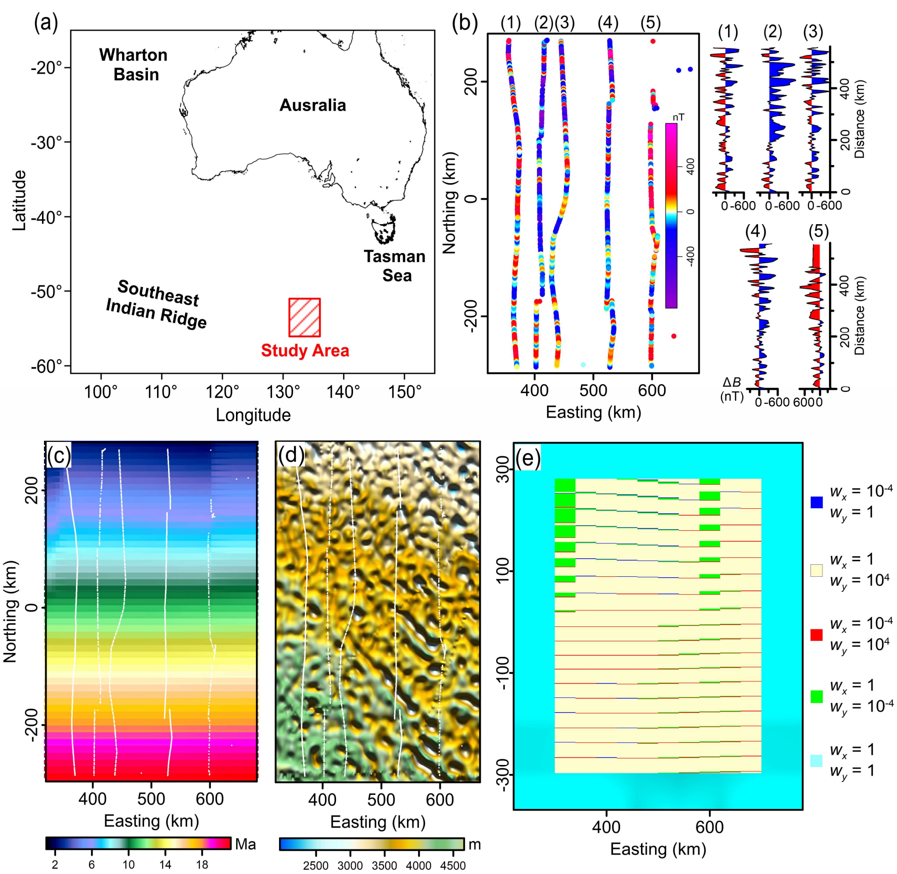

https://doi.org/10.5194/se-2021-117
Preprint. Discussion started: 30 September 2021

Solid Earth Discussions

Figure 3. Observed magnetic anomaly data, crust age, and seafloor relief in the study area in the east of the Southeast Indian Ridge. (a) Location of the study area, (b) observed magnetic anomaly data (ΔB) based on five survey lines, (c) crust age, (d) seafloor relief (in depth) in the study area from ETOPO1, and (e) distributions of ES cells in shallow (inside box) and deep (outside box) layers and their weights.

For illustrating the availability of proposed method to predict magnetic field, some observed data from survey lines (Figures 4) are extracted as verification data which are not included in the calculation. A dual-layer ES model was constructed using observed data to generate the magnetic anomaly map for the study area. The shallow layer composed of cells with a prism size of 1 km (in the south–north direction) × 40 km (in the west–east direction) × 1 km (in the depth direction) was placed on the surface beneath the seabed and close to the seafloor relief. The deep layer composed of cells with sizes of 80 km × 80 km × 40 km was placed on the surface close to the depth of the Curie point, which was estimated based on the transformation of the oceanic crust age (Yoshii, 1975). The ES cell ranges in the horizontal directions and their weights are shown in Figure 3e.

The magnetic anomalies at the verification points are predicted by ES model and compared with the observed values. The absolute errors (Figures 4) between these two data sets indicate that the prediction of magnetic anomaly can be considered effective. The magnetic map is create by using whole observed data to consructe ES model, which take into account the measured information and crust age information well (Figures 5a and d). Comparing the WDMAMv2 (Lesur et al., 2016) and EMAG2v3 (Meyer et al., 2017) models (Figures 5b and c) with observed data, significant differences between them can be seen in Figures 5e and f. Therefore, the

https://doi.org/10.5194/se-2021-117
Preprint. Discussion started: 30 September 2021

proposed method can be used to update above models in a global context. For instance, the data of WDMAMv2 (or EMAG2v3) and observed data can be fused through proposed method to obtain a new magnetic map.

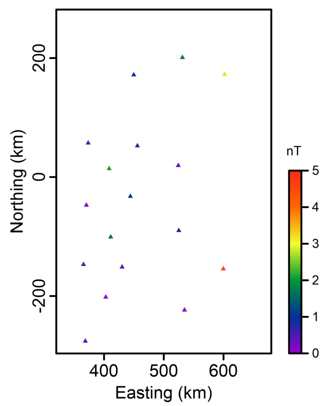

Figure 4. The absolute errors at verification points between the observed data and the predicted data.

https://doi.org/10.5194/se-2021-117
Preprint. Discussion started: 30 September 2021

Solid Earth
Discussions

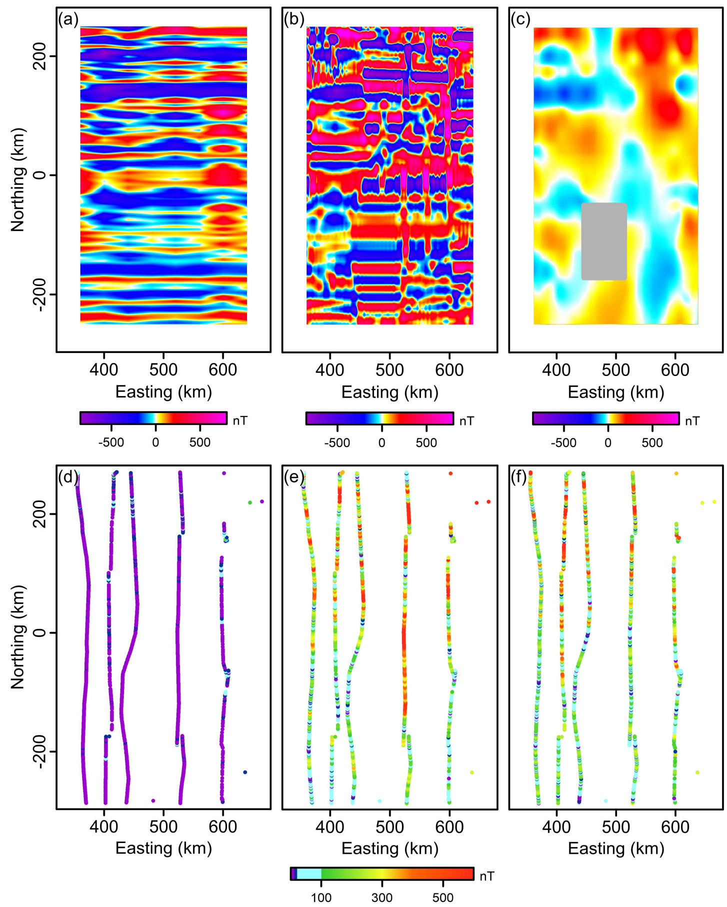

Figure 5. Magnetic anomaly maps with absolute errors for the observed points. (a) Magnetic anomaly (ΔB) map generated based on our method, (b) and (c) Magnetic anomaly maps based on the WDMAMv2 and EMAG2v3 models (grey area: no data available), respectively; (d), (e), and (f) Absolute errors of the observed data corresponding to the magnetic anomaly maps.

5 Conclusions

Interpolation techniques based on the morphological characteristics of data might not be suitable for areas with sparse observation data. The use of ES techniques may improve the interpolation of gravity and magnetic fields in areas with sparse data.

https://doi.org/10.5194/se-2021-117
Preprint. Discussion started: 30 September 2021

Solid Earth Discussions
Open Access

Additional geological information is required. The information was transformed as constraints added to the inversion by applied a model objective function. Many types of geological data, such as the oceanic crust age, can be transformed into constraints. The reasonable construction of an ES model can efficiently balance the effects of the background magnetic field on the prediction of the total magnetic field. The application of real data obtained for the Southeast Indian Ridge illustrates the effectiveness of our method. The result gives a good consideration to both the extension of the magnetic lineation feature and measured information. A crust age or seafloor relief with high spatial resolution are beneficial for the performance of the interpolation method.

Data availability. A set of synthetic test data presented herein are available from https://dx.doi.org/10.17632/p9xxchmwx7.1.

Author contributions. DL performed the numerical experiments and practical application with the analysis of calculation accuracy, and wrote the paper. JD, CC, QL, and SS joined the analysis, as well as discussed, commented on, and revised the manuscript.

Competing interests. The authors declare that they have no conflict of interest.

Acknowledgements. The authors are grateful to thank editor as well as the anonymous reviewers for their constructive feedback that helped us strengthen the manuscript.

Financial support. This work has been supported by the National Natural Science

Foundation of China (No. 42174090).

References

Bowles, J. A., Morris, A., Tivey, M. A. and Lascu, I.: Magnetic mineral populations in lower oceanic crustal gabbros (Atlantis Bank, SW Indian Ridge): Implications for marine magnetic anomalies, Geochemistry, Geophysics, Geosystem, 21, e2019GC008847, https://doi.org/10.1029/2019GC008847, 2020.

Briggs, I. C.: Machine contouring using minimum curvature, Geophysics, 39(1), 39–48, https://doi.org/10.1190/1.1440410, 1974.

Cooper, G. R. J.: Gridding gravity data using an equivalent layer, Computers & Geosciences, 26(2), 227–233, https://doi.org/10.1016/S0098-3004(99)00089-9, 2000.

Cooper, G. R. J. and Cowan, D. R.: Edge enhancement of potential-field data using normalized statistics. Geophysics, 71(3), H1–H4, https://doi.org/10.1190/1.2837309, 2008.

Cordell, L.: A scattered equivalent-source method for interpolation and gridding of potential-field data in three dimensions, Geophysics, 57(4), 629–636, https://doi.org/10.1190/1.1443275, 1992.

Dampney, N. G.: The equivalent source technique, Geophysics, 34(1), 39–53, https://doi.org/10.1190/1.1439996, 1969.

Demirel, S., Alpar, B., Yaltirak, C., Vardar, D. and Kurt, H.: Northern segment of the North Anatolian Fault in the Gulf of Izmit inferred from marine magnetic anomalies, Marine Geophysical Research, 41(1), 6, https://doi.org/10.1007/s11001-020-09399-6, 2020.

Granot, R., Dyment, J. and Gallet, Y.: Geomagnetic field variability during the

https://doi.org/10.5194/se-2021-117
Preprint. Discussion started: 30 September 2021

Cretaceous Normal Superchron, Nature Geoscience, 5(3), 220–223, https://doi.org/10.1038/N GEO1404, 2012.

Granot, R. and Dyment, J.: The influence of post-accretion sedimentation on marine magnetic anomalies. Geophysical Research Letters, 46, 4645–4652, https://doi.org/10.1029/2019GL082265, 2019.

Hansen, R. O.: Interpretive gridding by anisotropic kriging, Geophysics, 58(10), 1491–1497, https://doi.org/10.1190/1.1443363, 1993.

Krige, D. G.: A statistical approach to some basic mine valuation problems on the Witwatersrand, Journal of the Southern African Institute of Mining and Metallurgy, 52(6), 119–139, 1951.

Lelièvre, P. G. and Oldenburg, D. W.: A comprehensive study of including structural orientation information in geophysical inversions, Geophysical Journal International, 178(2), 623–637, https://doi.org/10.1111/j.1365-246X.2009.04188.x, 2009.

Lesur, V., Hamoudi, M., Choi, Y., Dyment, J. and Thébault E.: Building the second version of the World Digital Magnetic Anomaly Map (WDMAM), Earth, Planets and Space, 68, 27, https://doi.org/10.1186/s40623-016-0404-6, 2016.

Li, D., Liang, Q., Du, J., Sun, S., Zhang, Y., and Chen, C.: Transforming Total-Field magnetic anomalies into three components using dual-layer equivalent sources, Geophysical Research Letters, 47(3), e2019GL084607, https://doi.org/10.1029/2019 GL084607, 2020.

Li, Y. and Oldenburg, D. W.: 3-D inversion of magnetic data, Geophysics, 61(2), 394–408, https://doi.org/10.1190/1.1443968, 1996.

Li, Y. and D. W. Oldenburg, D. W.: Incorporating geologic dip information into geophysical inversions, Geophysics, 65(1), 148–157,

https://doi.org/10.5194/se-2021-117
Preprint. Discussion started: 30 September 2021

https://doi.org/10.1190/1.1444705, 2000.

Maher, S. M., Gee, J. S., Doran, A. K., Cheadle, M. J., and B. E. John, B. E.: Magnetic structure of fast-spread oceanic crust at Pito Deep, Geochemistry, Geophysics, Geosystem, 21, e2019GC008671, https://doi.org/10.1029/2019GC008671, 2020.

Maus, S., Barckhausen, U., Berkenbosch, H., Bournas, N., Brozena, J., Childers,V., Dostaler, F., Fairhead, J. D., Finn, C., von Frese, R. R. B., Gaina, C., Golynsky, S., Kucks, R., Lühr, H., Milligan, P., Mogren, S., Müller, R. D., Olesen, O., Pilkington, M., Saltus, R., Schreckenberger, B., Thébault, E., Caratori Tontini, F.: EMAG2: A 2-arc min resolution Earth Magnetic Anomaly Grid compiled from satellite, airborne, and marine magnetic measurements, Geochemistry, Geophysics, Geosystems, 10(8), Q08005, https://doi.org/10.1029/2009GC002471, 2009.

Meshram, S. G., Powar, P. L., Singh, V. P., and Meshram, C.: Application of cubic spline in soil erosion modeling from Narmada Watersheds, India, Arabian Journal of Geosciences, 11(13), 362, https://doi.org/10.1007/s12517-018-3699-8, 2018.

Meyer, B., Chulliat, A. and Saltus, R.: Derivation and error analysis of the Earth Magnetic Anomaly Grid at 2 arc min resolution version 3 (EMAG2v3), Geochemistry, Geophysics, Geosystems, 18(12), 4522–4537, https://doi.org/10.1002/2017GC 007280, 2017.

Müller, R. D., Sdrolias, M., Gaina, G. and Roeat, W. R.: Age, spreading rates, and spreading asymmetry of the world's ocean crust, Geochemistry, Geophysics, Geosystems, 9(4), Q04006, https://doi.org/10.1029/2007GC001743, 2008.

Paoletti, V., Ialongo, S., Florio, G., Fedi, M. and Cella, F.: Self-constrained inversion of potential fields, Geophysical Journal International, 195(2), 854–869, https://doi.org/10.1093/gji/ggt313, 2013.

https://doi.org/10.5194/se-2021-117
Preprint. Discussion started: 30 September 2021

Solid Earth Discussions
Open Access

Quesnel, Y., Catalán, M. and Ishihara, T.: A new global marine magnetic anomaly data set, Journal of Geophysical Research, 114, B04106, https://doi.org/10.1029/2008JB006144, 2009.

Sager, W. W., Weiss, C. J., Tivey, M. A. and Johnson, H. P.: Geomagnetic polarity reversal model of deep-tow profiles from the Pacific Jurassic Quiet Zone, Journal of Geophysical Research, 103(B3), 5269–5286, https://doi.org/10.1029/97JB03404, 1998.

Sayanagi, K. and Tamaki, K.: Database of marine magnetic-anomalies in the northeast Pacific, Atlantic, and southeast Indian oceans, Journal of Geomagnetism and Geoelectricity, 44(2), 143–160, https://doi.org/10.5636/jgg.44.143, 1992.

Shahbeik, S., Afzal, P., Moarefvand, P. and Qumarsy, M.: Comparison between ordinary kriging (OK) and inverse distance weighted (IDW) based on estimation error. Case study: Dardevey iron ore deposit, NE Iran, Arabian Journal of Geosciences, 7(9), 3693–3704, https://doi.org/10.1007/s12517-013-0978-2, 2014.

Sun, S. and Chen, C.: A self-constrained inversion of magnetic data based on correlation method, Journal of Applied Geophysics, 135, 8–16, https://doi.org/10.1016/j.jappg eo.2016.09.022, 2016.

Thébault, E., Finlay, C. C., Beggan, C. D., Alken, P., Aubert, J., Barrois, O., Bertrand, F., Bondar, T., Boness, A., Brocco, L., Canet, E., Chambodut, A., Chulliat, A., Coïsson, P., Civet, F., Du, A., Fournier, A., Fratter, I., Gillet, N., Hamilton, B., Hamoudi, M., Hulot, G., Jager. T., Korte, M., Kuang, W., Lalanne, X., Langlais, B., Léger, J., Lesur, V., Lowes, F. J., Macmillan, S., Mandea, M., Manoj, C., Maus, S., Olsen, N., Petrov, V., Ridley, V., Rother, M., Sabaka, T. J., Saturnino, D., Schachtschneider, R., Sirol, O., Tangborn, A., Thomson, A., Tøffner-Clausen, L., Vigneron, P., Wardinski, I. and T. Zvereva, T.: International Geomagnetic

https://doi.org/10.5194/se-2021-117
Preprint. Discussion started: 30 September 2021

Reference Field: the 12th generation, Earth Planets Space 67, 79, https://doi.org/10.1186/s40623-015-0228-9, 2015.

Tominaga, M., Sager, W. W., Tivey, M. A. and Lee, S. M.: Deep-tow magnetic anomaly study of the Pacific Jurassic Quiet Zone and implication for the geomagnetic polarity reversal timescale and geomagnetic field behavior, Journal of Geophysical Research, 113(B7), B07110, https://doi.org/10.1029/2007JB005527, 2008.

Tontini, F. C., Bassett, D., de Ronde, C. E. J., and Timm, C.: Early evolution of a young back-arc basin in the Havre Trough, Nature Geoscience, 12(10), 856–862, https://doi.org/10.1038/s41561-019-0439-y, 2019.

Vine, F. J. and Matthews, D. H.: Magnetic anomalies over oceanic ridges, Nature, 199(4897), 947–949, https://doi.org/10.1038/199947a0, 1963.

Xia, J., Sprowl, D. R., and Adkins-Heljeson, D.: Correction of topographic distortions in potential-field data: A fast and accurate approach, Geophysics, 58(4), 515–523, https://doi.org/10.1190/1.1443434, 1993.

Yoshii, T.: Regionality of group velocities of Rayleigh waves in the Pacific and thickening of the plate, Earth and Planetary Science Letters, 25(3), 305–312, https://doi.org/10.1016/0012-821X(75)90246-0, 1975.